



University
of Glasgow

Donaldson, R. J., Collins, R. J., Eleftheriadou, E., Barnett, S. M., Jeffers, J., and Buller, G. S. (2015) Experimental implementation of a quantum optical state comparison amplifier. *Physical Review Letters*, 114(12), 120505

Copyright © 2015 The American Physical Society

This work is made available under the Creative Commons Attribution 3.0 License (CC BY 3.0)

Version: Published

<http://eprints.gla.ac.uk/104517/>

Deposited on: 30 March 2015

Experimental Implementation of a Quantum Optical State Comparison Amplifier

Ross J. Donaldson,¹ Robert J. Collins,¹ Electra Eleftheriadou,² Stephen M. Barnett,³
John Jeffers,² and Gerald S. Buller¹

¹*SUPA, Institute of Photonics and Quantum Sciences, School of Engineering and Physical Sciences,
Heriot Watt University, David Brewster Building, Edinburgh EH14 4AS, United Kingdom*

²*SUPA, Department of Physics, University of Strathclyde, John Anderson Building,
107 Rottenrow, Glasgow G4 0NG, United Kingdom*

³*SUPA, School of Physics and Astronomy, University of Glasgow, Kelvin Building,
University Avenue, Glasgow G12 8QQ, United Kingdom*

(Received 25 August 2014; revised manuscript received 26 November 2014; published 26 March 2015)

We present an experimental demonstration of a practical nondeterministic quantum optical amplification scheme that employs two mature technologies, state comparison and photon subtraction, to achieve amplification of known sets of coherent states with high fidelity. The amplifier uses coherent states as a resource rather than single photons, which allows for a relatively simple light source, such as a diode laser, providing an increased rate of amplification. The amplifier is not restricted to low amplitude states. With respect to the two key parameters, fidelity and the amplified state production rate, we demonstrate significant improvements over previous experimental implementations, without the requirement of complex photonic components. Such a system may form the basis of trusted quantum repeaters in nonentanglement-based quantum communications systems with known phase alphabets, such as quantum key distribution or quantum digital signatures.

DOI: [10.1103/PhysRevLett.114.120505](https://doi.org/10.1103/PhysRevLett.114.120505)

PACS numbers: 03.67.Hk, 03.67.Ac, 42.50.Ar, 42.60.Da

Classical electromagnetic signals can, in principle, be amplified by any gain factor without being compromised by noise, allowing transmission losses to be overcome and signals to be transmitted further. Many systems transmitting signals using quantum states (e.g., quantum key distribution, QKD [1], or quantum digital signatures [2,3]) could benefit from amplification. Unfortunately, perfect deterministic amplification of an unknown quantum optical signal is impossible [4]. Any attempt to amplify introduces noise—the minimum amount of which is limited by the uncertainty principle [5]—overwhelming any quantum properties that the signal has. For example, an erbium doped fiber amplifier introduces noise via the spontaneous emission process [6].

Nondeterministic amplifiers work in postselection [7]—the amplified output is accepted conditional on a measurement outcome, or otherwise discarded. The original scheme was based on the quantum-scissors device [8] and further protocols were proposed [9–12], some based on photon addition and subtraction [9] and on noise addition and photon subtraction [10,11]. Several were later experimentally realized [13–17]. Each scheme has advantages and disadvantages. The quantum-scissors- and

photon-addition-based experiments require single-photon sources, limiting high-fidelity output to a set of states with limited overlap with the two-photon state. Cascading devices would circumvent this limitation, as would using quantum scissors with two photons as input [11]. Single-photon generation is still a challenging proposition that offers low photon fluxes [18], and the success probability is low, making cascading impractical. Research continues into improving heralded photon source amplifiers for measurement device independent QKD [19–21]. The noise-addition scheme removes the requirement for single photons and works well as a phase concentrator, but the fidelity of the output state compared to a perfectly amplified version of the input state is typically low [10,12,16]. For example, for a coherent state with mean input photon number of 0.25 and an intensity gain of twofold, the theoretical fidelity of the output to the target amplified state is ≈ 0.8 , while the vacuum state has a fidelity of more than 0.6 with the target. Generally, these systems exhibit a trade-off between fidelity and gain.

Here, we demonstrate experimentally our protocol [22] that, using coherent light sources, linear optical components, and commercial photodetectors, can amplify coherent states of any experimentally reasonable amplitude chosen from a limited set, using the established techniques of nondemolition comparison [23] and photon subtraction [24]. The operation of the experiment is shown in Fig. 1 [25]. Beam splitter BS1 and detector D_0 perform the comparison between an input coherent state to be amplified

Published by the American Physical Society under the terms of the *Creative Commons Attribution 3.0 License*. Further distribution of this work must maintain attribution to the author(s) and the published article's title, journal citation, and DOI.

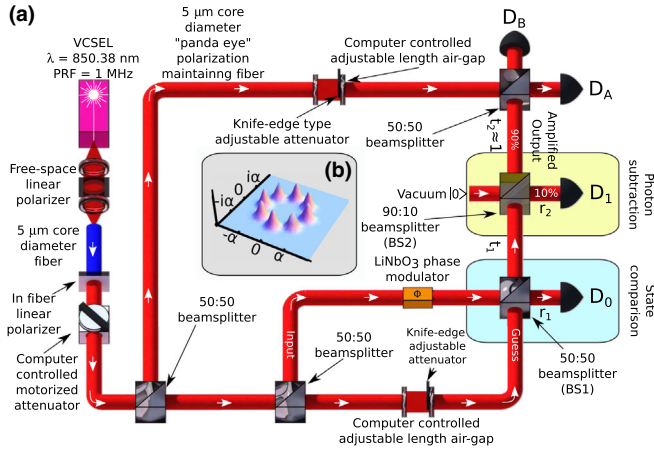


FIG. 1 (color online). (a) Experimental implementation of the quantum optical state comparison amplifier and output state analyzer. The system comprises two interferometers. Each D denotes a silicon single-photon detector [30]; VCSEL denotes a vertical cavity surface emitting laser and PRF the pulse repetition frequency of the laser. (b) Eight possible input coherent states.

(chosen randomly from a known set) and a selected guess state. Guess states are chosen randomly from a set so that each interferes destructively with one of the possible input states to produce a vacuum state at D_0 . For known transmission alphabets it is logical to limit the alphabet of the guess. If the guess is correct, the transmitted fraction of the input state interferes destructively with the reflected fraction of the guess state, D_0 does not fire (assuming no spurious counts), and the light passes BS2. For incorrect guesses some light leaks into D_0 , where it may or may not cause a count, as low amplitude states have a large overlap with the vacuum. The nonfiring of D_0 is taken as an *imperfect* indication that the guess and input states are matched.

The postselected output of the comparison beam splitter is a reasonable, approximate version of the amplified input state but inclusion of a second stage, comprising a highly transmitting beam splitter BS2 and a detector D_1 to perform photon subtraction, improves the fidelity. A small fraction of the incident light is reflected into D_1 . When this detector fires it is likely that the output of the first interferometer was of a higher mean photon number. This increases the purity of the output state, cleaning it of lower mean photon number states produced by incorrect guesses at the comparison stage. The nominal gain of the whole device is $g = t_2/r_1$ (see Fig. 1).

Our approach has similarities, but also differences, with the schemes mentioned earlier. We rely on the addition of coherent light to the input using a beam splitter, similar to Ref. [17]. Unlike quantum-scissors-based devices that require single photons, or incoherent devices that use noisy fields, ours is designed to exploit the phase coherence of coherent states. Its operation relies on the interference of the input and guess coherent states and it will not work

significantly for an incoherent guess state. It is therefore fundamentally different to the noise-addition approach, where the noise is an incoherent source [10,16] and a phase reference between the state to be amplified and the noise field is not necessary [10,16,17]. Noise-addition experiments use photon number resolving detectors to improve the fidelity while our approach operates with simpler single-photon triggering detectors. These are the main differences and simplifications that give our method an advantage [10,16,20].

We generate input states by attenuating the output of a diode laser [25] to the desired mean photon number per pulse $|\alpha|^2$, where α is the coherent amplitude. These states are fed into a system comprised of two interferometers assembled from 5 μm core diameter polarization maintaining fiber [31], the outer of which performs an analysis measurement on the amplified states by interfering the output states with a copy of the target state $|g\alpha\rangle$ with a classical visibility of 92.24% at detectors D_A and D_B .

In the current realization the states are interfered at a 50:50 beam splitter, so the input and guess sets have the same mean photon number. Experimental imperfections mean that the phase profile of the guess consists of a narrow spread of phases centered on the expected value. The input also exhibits a slight spread of values (in our experiment $\pm 1.6 \times 10^{-3}$ radians). The inner interferometer and detector D_0 perform the state comparison with an unconditioned classical visibility of 92.41%. Photon subtraction is performed using BS2 (t_2)²:(r_2)² = 90:10, with the 10% reflecting to detector D_1 . Generation of an amplified state is heralded by the absence of a detection event at D_0 and the presence of a detection event at D_1 . Thus, our simple implementation produces a device with a uniform nominal intensity gain of 1.8 over a range of input amplitudes, unlike schemes based on photon addition and subtraction [9,15].

The quality of the amplified output depends on the set of possible input states. We choose coherent states with mean amplitudes selected symmetrically on circles in the Argand plane. We present results for input sets $\{|\alpha \exp(2m\pi/N)\rangle\}$, for $N = 2$, $N = 4$, and $N = 8$, with $m = 0, \dots, N - 1$. The results for the last two of these sets approach closely those of the phase-covariant set covering the entire circle.

In Fig. 2(a) we show the outer analysis interferometer visibility for the two-state set as a function of input mean photon number. We plot separately the visibilities for the output of the amplifier in three cases: when it is fully unconditioned, conditioned only on state comparison (only on D_0 not firing), and conditioned on both comparison and subtraction (on both D_0 not firing and D_1 firing). As expected the state comparison works better with increasing mean photon numbers. The photon-subtraction step cleans the state further so that the visibility is nearly ideal. This almost-perfect output is only possible with a single subtraction stage as the subtraction effectively excludes the wrong state reaching the outer interferometer.

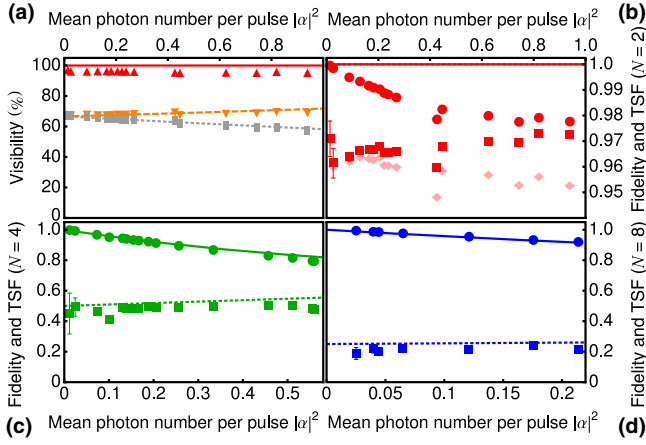


FIG. 2 (color online). (a) Experimental and fitted theoretical visibilities at the outer interferometer for $N = 2$. The dotted grey curve is for the unconditioned output, the dashed orange curve for output conditioned on D_0 not firing, and the solid red curve for D_0 not firing and D_1 firing. Typical standard error in the measurements is ± 0.05 . (b)–(d) Fraction of the target state in the output and fidelity. The subfigures represent the fractions of the target state in the output of the state comparison amplifier (squares) and the fidelity of the output state to the target state $|\alpha\rangle$ (dots) as a function of input photon number. (b) The two-state set, (c) the four-state set, and (d) the eight-state set. The $|\alpha|^2 = 0.0033$ point for the eight-state set has been omitted as the low number of overall counts renders this unreliable. In (b) the paler colored diamonds represent the partially conditioned case that considers only D_1 firing and ignores D_0 events. The standard error, shown for the correct state fraction, decays quickly with mean photon number. Standard errors for the fidelity are small: typically ± 0.0003 for $N = 2$, ± 0.0022 for $N = 4$, and ± 0.0013 for $N = 8$. Lines are theoretical best-fit curves based on experimental parameters.

Figures 2(b)–2(d) show the target output state fraction (TSF) and the output fidelities for $N = 2, 4$, and 8 . The state fraction is the proportion of times that the device produces the target state $|\alpha\rangle$. We calculate this from our measured counts using the procedure outlined in Sec. II of the Supplemental Material [25]. Without the conditioning imposed by the device for the two-, four-, and eight-state sets these percentages would be 50%, 25%, and 12.5%, but the amplification has increased these values to $>95\%$, $\approx 60\%$, and $\approx 30\%$, respectively.

As well as increasing the target state fraction the state comparison amplifier reduces the relative probabilities of states with amplitudes further from the target state. For the four- and eight-state sets this increases the fidelity without contributing to the target state fraction. For each set we provide an estimate of the fidelity of the output compared to the nominal target output state. The estimate is obtained on the basis that the device only produces a limited set of states and on the measured counts in the outer interferometer [25]. The detectors were operated in Geiger mode [18] and therefore output a fixed electrical signal irrespective of the

number of photons in a nonvacuum pulse, resulting in a reduced fidelity at larger $|\alpha|^2$ [25].

The plots show that the fidelity of the amplifier system presented here compares well with previous demonstrations of nondeterministic amplifiers. We emphasize that the theoretical performance of the state comparison amplifier for the phase-covariant input state set is similar to that for the four- and eight-state sets. For the four-state set the conditioning increases the fidelity from an expected value for unconditioned output of 0.65, for a mean input photon number of ≈ 0.5 , to >0.8 . For the eight-state set the unconditioned state should have a fidelity with the target state of 0.82 for a mean input photon number of 0.21. It is clear that the state comparison amplifier increases the value significantly, to >0.9 . For all three input state sets the fidelity is greatly increased across the whole range of photon numbers.

In the Supplemental Material [25] we provide a table which compares our amplifier with three previously implemented amplifiers, the scissors-based, noise-addition-based, and photon-addition- and subtraction-based amplifiers at similar gains and input mean photon numbers. These all have different characteristics, but we can summarize the results simply by saying that the state comparison amplifier provides a significantly higher fidelity than all of the other amplifiers if we restrict the alphabet to $N = 2$. This is mainly because the other implementations are phase covariant and so do not take advantage of limited bases. For $N = 4$ and $N = 8$ the photon-addition and subtraction amplifier can provide a slightly better fidelity than the state comparison amplifier. In the Supplemental Material [25] we also plot another figure of merit for our amplifier, the equivalent input noise. We find that it is negative, within the range disallowed for normal amplifiers.

In all cases our lack of complex quantum resources gives us an advantage over these amplifiers in terms of success rate. The nominal success probability of our device is high (comparable to other nondeterministic amplification methods), depending on the input mean photon number, the number of states in the set, and the operating parameters of the photon detectors, but this is not the main advantage of the state comparison amplifier. Because our amplifier uses only the light from a laser diode as a resource the high success probability translates into a high rate of real time success (Fig. 3) making high-quality transmission of quantum information at large data rates possible. For example, for the two-state set and $|\alpha|^2 = 0.94$, we obtain more than 26 ks^{-1} almost perfectly amplified states, corresponding to a measured success probability of 2.6% [22]. For perfectly efficient detectors and no internal losses the maximum theoretical success probability at this mean photon number is 9.9%. The rate can be increased by reducing losses or increasing the pulse repetition frequency (PRF). The technological limitation in our system is the count rate limit of the detectors. We can compare the

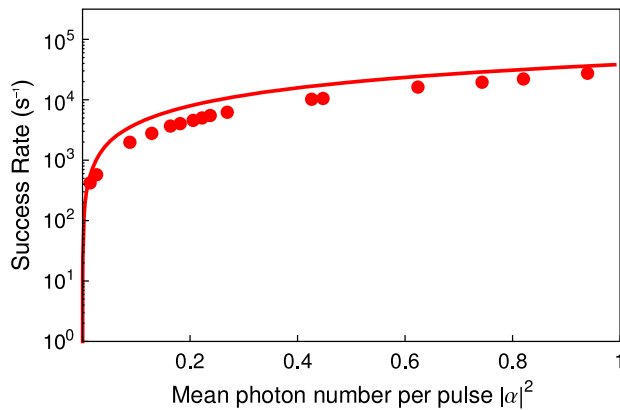


FIG. 3 (color online). The success rate of the amplifier corresponds to the gated count rate at the D_1 detector when D_0 does not fire and is shown for the two-state set as a function of input photon number. The success rates for the four- and eight-state sets follow that for $N = 2$ closely. The line represents a theoretical best-fit curve based on experimental parameters. As our laser clock rate is set at 1 MHz a success rate of 10^5 corresponds to an experimental success probability of 10%. Our maximum measured probability is 2.6%.

success rate to those in other amplifier experiments. Systems using down-conversion to produce single photons run at a relatively low rate of pair production. For example, in Ref. [13] the rate of pair production was 2.5 k s^{-1} , so the success probability of the scheme together with detection losses mean success rates will be significantly lower than this. The systems in Refs. [14,15] also use down-conversion, and so their rates will be of the same order. The success probability of the coherent noise addition/photon subtraction experiment is similar to ours for a single subtraction, but of course lower for multiple subtractions [17].

One further comparison that we can make is with a “classical amplifier” using unambiguous state discrimination (USD) [32–34] to determine the phase of the coherent states without error. This approach offers the potential of arbitrarily large amplification by creating coherent states with the same phase as the input states, but with any desired magnitude. In previous work [3] we have shown that experimental USD for $N = 4$ has a very small success probability for the same input amplitudes. This USD success probability decreases with increasing number of phases so the system presented here will always perform better by this measure.

Our system operates proficiently but could be improved if detectors D_0 and D_1 had higher quantum efficiency (QE). A wavelength of 850 nm was selected due to the availability of comparatively easy to operate high QE, low dark noise semiconductor photodetectors at this wavelength [18,35]. In this demonstration the mean QE across the detectors was 40.5%. As the main conditioning parameter is an event at D_1 , a low QE here results in the increased rejection of correctly amplified states while a high dark count rate will result in a fraction of the incorrectly amplified states being

mistakenly accepted. A low QE for D_1 has no effect on the fidelity for $N = 2$ and slightly improves the fidelity of the subtraction operation for $N = 4$ and $N = 8$. The cost is a reduced success rate.

The QE and dark count rate of D_0 are also important although the acceptance and rejection cases are reversed with respect to D_1 . Low efficiency of D_0 amounts to performing the state comparison with coherent states of lower amplitude, with increased vacuum components. It therefore reduces the comparison effect by rendering the compared quantum states less orthogonal. This decreases the fidelity for $N = 4$ and $N = 8$. The mean raw dark count rate of each detector was 296 s^{-1} which became 8 s^{-1} after gating. Thus, the mean dark count rate per pulse per detector is 8×10^{-6} , which is negligible for all reasonable input amplitudes.

The visibility of the interference process at BS1 in Fig. 1 also contributes to the efficiency of system operation. Poor visibility at BS1 will result in the incorrect rejection of correctly amplified states when conditioning at D_1 is taken into account. As visibilities can typically be made high in comparison to most values of QE the contribution is less significant.

In summary, we demonstrated a simple method of amplifying coherent states with high fidelity and success rate unsurpassed by other methods. Previous experimental demonstrations of nondeterministic amplifiers used added random noise or required complex resources like single-photon sources or photon number resolving detectors, whereas we use coherent states and commercially available single-photon detectors. A significant advantage of the system is that the rate of successful operation of the amplifier is the product of the amplifier success probability and the PRF of the laser—a feature that nondeterministic amplifiers based on the addition of single photons cannot replicate without the development of a rapid-fire synchronizable source.

The system could be improved to operate at higher gains by using a lower reflectivity BS1, at cost to the fidelity. The gain would increase since a greater fraction of the input and guess state amplitudes would reach the unmeasured output of BS1. The success rate is largely determined by the photon-subtraction rate, which is proportional to the intensity in this arm, so this would increase too. The consequent drop in fidelity would occur because the amplitude of the fraction of incorrect states in the output of BS1 would increase. Thus the incorrect fraction would more frequently pass the photon-subtraction test. The fidelity reduction can be offset by the inclusion of multiple photon-subtraction stages, a technique shown to be effective in other experiments [16]. BS2 controls both the gain and success rate, but not fidelity. Higher transmission provides higher gain, but lower success rate, and vice versa.

The system has many possible applications. It could be used in the sharing of quantum phase references [36].

Additionally, it could operate as a trusted quantum repeater in nonentanglement-based quantum communications systems with known phase alphabets, such as QKD [1] or quantum digital signatures [2,3], increasing the transmission distance of such systems.

This work was supported by the Royal Society (U.K.), the Wolfson Foundation (U.K.), and the U.K. Engineering and Physical Sciences Research Council (EPSRC) through both Platform Grant No. EP/K015338/1 and the Quantum Communications Hub Grant No. EP/M013472/1.

-
- [1] N. Lütkenhaus and A. J. Shields, *New J. Phys.* **11**, 045005 (2009).
- [2] P. J. Clarke, R. J. Collins, V. Dunjko, E. Andersson, J. Jeffers, and G. S. Buller, *Nat. Commun.* **3**, 1174 (2012).
- [3] R. J. Collins, R. J. Donaldson, V. Dunjko, P. Wallden, P. J. Clarke, E. Andersson, J. Jeffers, and G. S. Buller, *Phys. Rev. Lett.* **113**, 040502 (2014).
- [4] H. A. Haus and J. A. Mullen, *Phys. Rev.* **128**, 2407 (1962).
- [5] C. M. Caves, *Phys. Rev. D* **26**, 1817 (1982).
- [6] A. W. Naji and B. A. Hamida, *Int. J. Phys. Sci.* **6**, 4674 (2011).
- [7] T. C. Ralph and A. P. Lund, in *Proceedings of the 9th International Conference on Quantum Communication Measurement and Computing*, edited by A. Lvovsky (AIP, Melville, NY, 2009), p. 155.
- [8] D. T. Pegg, L. S. Phillips, and S. M. Barnett, *Phys. Rev. Lett.* **81**, 1604 (1998).
- [9] J. Fiurášek, *Phys. Rev. A* **80**, 053822 (2009).
- [10] P. Marek and R. Filip, *Phys. Rev. A* **81**, 022302 (2010).
- [11] J. Jeffers, *Phys. Rev. A* **82**, 063828 (2010).
- [12] J. Jeffers, *Phys. Rev. A* **83**, 053818 (2011).
- [13] G. Xiang, T. Ralph, A. Lund, N. Walk, and G. Pryde, *Nat. Photonics* **4**, 316 (2010).
- [14] F. Ferreyrol, M. Barbieri, R. Blandino, S. Fossier, R. Tualle-Brouiri, and P. Grangier, *Phys. Rev. Lett.* **104**, 123603 (2010).
- [15] A. Zavatta, J. Fiurášek, and M. Bellini, *Nat. Photonics* **5**, 52 (2011).
- [16] M. A. Usuga, C. R. Müller, C. Wittmann, P. Marek, R. Filip, C. Marquardt, G. Leuchs, and U. L. Andersen, *Nat. Phys.* **6**, 767 (2010).
- [17] C. R. Müller, C. Wittmann, P. Marek, R. Filip, C. Marquardt, G. Leuchs, and U. L. Andersen, *Phys. Rev. A* **86**, 010305 (2012).
- [18] G. S. Buller and R. J. Collins, *Meas. Sci. Technol.* **21**, 012002 (2010).
- [19] N. Bruno, V. Pini, A. Martin, and R. Thew, [arXiv:1306.3425v1](https://arxiv.org/abs/1306.3425v1).
- [20] N. Gisin, S. Pironio, and N. Sangouard, *Phys. Rev. Lett.* **105**, 070501 (2010).
- [21] D. Pitkanen, X. Ma, R. Wickert, P. van Loock, and N. Lütkenhaus, *Phys. Rev. A* **84**, 022325 (2011).
- [22] E. Eleftheriadou, S. M. Barnett, and J. Jeffers, *Phys. Rev. Lett.* **111**, 213601 (2013).
- [23] A. Chefles, E. Andersson, and I. Jex, *J. Phys. A* **37**, 7315 (2004).
- [24] J. Wenger, R. Tualle-Brouiri, and P. Grangier, *Phys. Rev. Lett.* **92**, 153601 (2004).
- [25] See Supplemental Material at <http://link.aps.org/supplemental/10.1103/PhysRevLett.114.120505> for full details of the experimental methods, an estimation of the fidelity from interferometric photon counts, and a more detailed comparison of device performance with other examples from the literature, which includes Refs. [26–29].
- [26] P. J. Clarke, R. J. Collins, P. A. Hiskett, M.-J. García-Martínez, N. J. Krichel, A. McCarthy, M. G. Tanner, J. A. O'Connor, C. M. Natarajan, S. Miki *et al.*, *New J. Phys.* **13**, 075008 (2011).
- [27] M. Wahl, H.-J. Rahn, T. Röhlicke, G. Kell, D. Nettels, F. Hillger, B. Schuler, and R. Erdmann, *Rev. Sci. Instrum.* **79**, 123113 (2008).
- [28] K. J. Gordon, V. Fernandez, G. S. Buller, I. Rech, S. D. Cova, and P. D. Townsend, *Opt. Express* **13**, 3015 (2005).
- [29] C. I. Osorio, N. Bruno, N. Sangouard, H. Zbinden, N. Gisin, and R. T. Thew, *Phys. Rev. A* **86**, 023815 (2012).
- [30] A. Spinelli, L. M. Davis, and H. Dautet, *Rev. Sci. Instrum.* **67**, 55 (1996).
- [31] A. Kumar and A. Ghatak, *Polarization of Light with Applications in Optical Fibers*, 1st ed. (SPIE-International Society for Optical Engineering, Bellingham, WA, 2011), Vol. TT90.
- [32] V. Dunjko and E. Andersson, *Phys. Rev. A* **86**, 042322 (2012).
- [33] M. Sedláč, M. Ziman, O. Příbyla, V. Bužek, and M. Hillery, *Phys. Rev. A* **76**, 022326 (2007).
- [34] L. Bartůšková, A. Černoč, J. Soubusta, and M. Dušek, *Phys. Rev. A* **77**, 034306 (2008).
- [35] R. J. Collins, R. H. Hadfield, and G. S. Buller, *J. Nanophoton.* **4**, 040301 (2010).
- [36] S. D. Bartlett, T. Rudolph, and R. W. Spekkens, *Rev. Mod. Phys.* **79**, 555 (2007).